A comparison of the UCD/CIT air quality model and the CMB source–receptor model for primary airborne particulate matter

Tony Held[a], Qi Ying[a], Michael J. Kleeman[a,*], James J. Schauer[b], Matthew P. Fraser[c]

[a]Department of Civil and Environmental Engineering, University of California, 1 Shields Ave, Davis, CA 95616, USA
[b]Department of Civil and Environmental Engineering, University of Wisconsin-Madison, 600 N. Park St., Madison, WI 53706, USA
[c]Department of Civil and Environmental Engineering, Rice University, 6100 Main St., Houston, TX 77005, USA

Abstract

Source contributions to primary airborne particulate matter calculated using the source-oriented UCD/CIT air quality model and the receptor-oriented chemical mass balance (CMB) model are compared for two air quality episodes in different parts of California. The first episode occurred in the San Joaquin Valley on 4–6 January 1996, with peak 24 h average PM2.5 concentrations exceeding $100 \mu g \, m^{-3}$. This episode was characterized by low photochemical activity and high particulate nitrate concentrations, with localized regions of high particulate carbon concentrations around urban centers. The second episode occurred in the South Coast Air Basin on 7–9 September 1993, with peak 4 h average PM2.5 concentrations reaching $86 \mu g \, m^{-3}$. This episode was characterized by high photochemical activity and high secondary organic aerosol concentrations. The results from the two independent source apportionment calculations show strong agreement for source contributions to primary PM2.5 total organic mass at 7 receptor sites across the two studies, with a correlation slope of 0.84 and a correlation coefficient (R^2) of 0.70. Agreement for source contributions to primary PM2.5 total mass was similarly strong, with a correlation slope of 0.83 and a correlation coefficient (R^2) of 0.55. Wood smoke was identified as the dominant source of primary PM2.5 at urban locations in the SJV by both source apportionment techniques. Transportation sources including paved road dust, gasoline engines, and diesel engines, were identified as the dominant source of primary PM2.5 at all locations in the SoCAB by both models. The amount of secondary particulate matter (organic and inorganic) was in good agreement with the measured values minus the primary material identified by the CMB calculation.

The UCD/CIT air quality model is able to predict source contributions to airborne particulate matter at all locations and times throughout the study domain. The regional plots of source contributions to primary PM2.5 mass concentrations generated by the UCD/CIT air quality model suggest that high concentrations ($25 \mu g \, m^{-3}$) of primary PM2.5 mass released from the combustion of fuel with high sulfur content exist in areas adjacent to the Los Angeles

*Corresponding author. Tel.: +1 530 752 8386; fax: +1 530 752 7872.
E-mail address: mjkleeman@ucdavis.edu (M.J. Kleeman).

International Airport and the port of Los Angeles. Emissions profiles for these sources should be developed so that they can be included in future CMB calculations.

1. Introduction

Preliminary data indicate that large regions in the United States have ambient PM2.5 concentrations that exceed the new PM2.5 NAAQS resulting in unhealthy conditions for a significant fraction of the population in North America (Bae et al., 2004; Butler et al., 2003; Modey and Eatough, 2004; Russell et al., 2004; Watson and Chow, 2002; Wittig et al., 2004). Air quality managers at the national, state, and local levels will soon need to characterize their particulate air quality problems and devise a strategy to reduce PM2.5 concentrations to comply with new standards. One of the most popular tools currently used to quantify source contributions to airborne particulate matter is the chemical mass balance (CMB) model. The CMB model identifies source contributions to primary particulate matter at specific receptor sites where PM composition measurements are available. The model is relatively easy to apply since it has a low computation burden and it does not require information about meteorological conditions or emissions inventories. CMB calculations have been carried out in numerous studies around the world (Abu-Allaban et al., 2002; Chen et al., 2001; Chow et al., 1992; Park et al., 2001; Watson et al., 2001, 2002; Zheng et al., 2002).

While the CMB model is robust and relatively easy to apply, it does not provide all the information that may be needed to formulate an effective PM2.5 control plan to protect public health in a typical airshed. Localized regions of high particulate matter concentrations often exist in airsheds that cannot be identified by the CMB model unless measurements are made at very fine spatial resolution. This ''saturation'' measurement approach becomes prohibitively expensive using current technology. The CMB model also does not identify sources of secondary particulate matter. In many regions across the United States, secondary particulate matter accounts for more than 50% of the PM2.5 concentrations during severe particulate air quality episodes (Kim et al., 2000a, b; Vukovich and Sherwell, 2002). A complimentary approach to the CMB model that could predict sharp gradients in source contributions to particulate matter concentration and that could predict source contributions to secondary particulate matter would be very helpful.

Recently, a reactive chemical transport model (CTM) with source apportionment capabilities has been demonstrated that fulfills some of the needs described above (Kleeman and Cass, 2001). The UCD/CIT source-oriented external mixture air quality model has been used to predict source contributions to the regional distribution of primary and secondary particulate matter in the San Joaquin Valley (SJV) and the South Coast Air Basin (SoCAB) during multiple air quality episodes (Held et al., 2004; Kleeman and Cass, 2001; Ying et al., submitted for publication; Ying and Kleeman, submitted for publication). CMB calculations were also performed for several of these episodes, enabling a direct comparison of these different source apportionment methods. This consistency check will verify the performance of the UCD/CIT air quality model for primary particulate matter at specific receptor sites, leading to increased confidence in the basic source apportionment capabilities that act as the foundation for more advanced source apportionment features.

The purpose of this study is to compare predicted source contributions to primary airborne particulate matter calculated using the UCD/CIT air quality model and the CMB model. A brief overview of each model will be provided, along with a description of the air quality episodes that were studied. Source contributions to primary particulate PM2.5 total organic mass concentrations and primary particulate PM2.5 total mass concentrations will then be compared. Finally, the regional distribution of primary particulate matter predicted by the UCD/CIT air quality model will be examined to identify sharp concentration gradients and sources that may have been missed by CMB calculations.

2. Model description

The CMB model uses measured source concentration profiles for primary particulate matter to identify source contributions to airborne particulate matter at a receptor location. The CMB model is expressed by the following set of linear equations:

$$c_{ik} = \sum_{j=1}^{m} a_{ij} s_{jk}, \tag{1}$$

where c_{ik} is the concentration of chemical species i in fine particles at receptor site k, a_{ij} is the relative concentration of chemical species i in fine particle emissions from

source j, and s_{jk} is the contribution that source j makes to fine particle mass at receptor site k. The model solves for source contributions s_{jk} that result in the predicted concentrations c_{ik} that best match measured concentrations at receptor site k. The model assumes that composition profiles are available for all significant emissions sources, and that chemical species used in source profiles do not undergo chemical transformation between the emissions source and the receptor site. Consistent methods for the measurement of chemical species must be used for source and receptor measurements to avoid biasing the calculation.

In the present study, results are used from two previous source–receptor applications (Schauer and Cass, 2000; Schauer et al., 2002a, b, c) that used trace organic compounds in addition to elements measured with XRF and organic compounds/ elemental carbon. Trace organic compounds that a re uniquely associated with an emissions source increase the resolution of CMB calculations. A total of 22 particle-phase chemical species were used for source apportionment calculations in the SJV episode, while 49 gas- and particle-phase species were used in the SoCAB episode. Additional details describing the CMB applications are provided in the references described above.

The UCD/CIT airshed model is a reactive CTM that predicts the evolution of gas- and particle-phase pollutants in the atmosphere in the presence of emissions, transport, deposition, chemical reaction, and phase change. The non-linear differential equation describing the evolution of species in the atmosphere is

$$\frac{\partial C_i}{\partial t} + \nabla \cdot u C_i = \nabla K \nabla C_i + E_i - S_i + R_i^{\text{gas}}(C) + R_i^{\text{part}}(C) + R_i^{\text{phase}}(C), \tag{2}$$

where C_i is the concentration of gas- or particle-phase species i at a particular location as a function of time t, u is the wind vector, K is the turbulent eddy diffusivity tensor (assumed to be diagonal), E_i is the emissions rate, S_i is the loss rate, R_i^{gas} is the change in concentration due to gas-phase reactions, R_i^{part} is the change in concentration due to particle-phase reactions, and R_i^{phase} is the change in concentration due to phase change. The model includes a gas-phase photochemical reaction mechanism that describes more than 100 gas-phase chemical species that play a role in the formation of ozone and other related pollutants. More than 50 particle-phase chemical species are included in each of 15 discrete particle sizes that span the range from 0.01 to 10 μm particle diameter.

The UCD/CIT airshed model represents airborne particles as a *source-oriented external mixture*. Particles released from different emissions source classes are tracked separately through the simulated atmosphere. The contribution that a source class makes to airborne particle concentrations at a downwind receptor site can be directly calculated from the model output. The model has the additional benefit of predicting how atmospheric processing alters the particles between the emissions location and the receptor site.

In the present study, UCD/CIT results are used from previous model applications (Held et al., 2004; Ying and Kleeman, submitted for publication). In both applications, meteorological data and initial/boundary concentrations were interpolated based on measurements. Emissions inventories for basic pollutants were supplied by the California Air Resources Board (SJV) or the South Coast Air Quality Management District (SoCAB) and then transformed into detailed modeling inventories using measured source profiles (Cooper et al., 1989; Harley et al., 1992, 1993; Hildemann et al., 1991a, b; Houck et al., 1989; Kleeman et al., 1999, 2000; Schauer et al., 1999a, b, 2001, 2002a, b, c; Taback et al., 1979). Gas-to-particle conversion and particle-phase chemistry for inorganic species were represented by the aerosol operators described by Kleeman and Cass (1998, 2001).

For the SJV episode of 4–6 January 1996, the study region was represented by a $54 \times 72 \times 5$ grid (west, north, vertical) with dimensions of 4 km, 4 km, and 39–429 m (lowest–highest). Gas-phase chemical reactions were modeled using the SAPRC90 chemical mechanism (Carter, 1990) with extensions to describe the formation of secondary organic aerosol (SOA) species (Kleeman and Cass, 2001) based on the gas-phase reactions described by Pandis et al. (1992) and the partitioning coefficients measured by Odum et al. (1996). The effect of temperature on SOA partitioning was considered using the techniques described by Aw and Kleeman (2003).

For the SoCAB episode of 7–9 September 1993, the study region was represented by a $80 \times 30 \times 5$ grid (west, north, vertical) with dimensions of 5 km, 5 km, and 39–429 m (lowest–highest). Gas-phase chemical reactions (including the production of secondary organic species) were modeled using the Caltech Atmospheric Chemistry Mechanism (CACM) (Griffin et al., 2002). The partitioning of secondary organic species to each discrete particle size/class was represented using Eq. (8) described by Kleeman et al. (Kleeman and Cass, 2001) and the thermodynamic data described by Pun et al. (2002). Only hydrophobic SOA species were considered in the present study since hydrophilic SOA species accounted for less than 10% of the total SOA concentration (Pun et al., 2002), but the calculation of these species adds considerable computational burden to the model. Additional details of these UCD/CIT model applications can be found in the references described above.

3. Summary of air quality episodes

During the period 4–6 January 1996, a high-pressure cell stagnated over the SJV causing generally stagnant wind conditions and elevated temperatures above the ground that reduced atmospheric mixing. These meteorological conditions are typical during winter air quality episodes in the SJV. Photochemical activity during the episode was low because the actinic flux was close to the annual minimum. As a result, peak 1 h average ozone concentrations were less than 50 ppb. Airborne particulate matter concentrations were large, reaching 24 h average values of more than $100 \, \mu g \, m^{-3}$ (Magliano et al., 1999). The composition of the airborne particles was dominated by ammonium nitrate, with high concentrations of carbonaceous particles measured around urban locations. Air quality measurements used to support CMB calculations were made at Fresno, Kern Wildlife Refuge, and Bakersfield in the SJV on 4–6 January 1996. The location of these receptor sites is shown in Fig. 7. Fresno and Bakersfield are the two largest cities in the SJV, while the Kern Wildlife Refuge is a rural site far removed from urban activities. The region around Fresno is dominated by agriculture, while the region around Bakersfield is dominated by oil refining. Fresno has one major transportation corridor passing through its boundaries (California State Highway 99) while Bakersfield has two major transportation corridors (Interstate 5 and California State Highway 99).

The air quality episode that occurred in the SoCAB on 7–9 September 1993 was a severe event. Stagnant winds combined with ambient temperatures that exceeded $40 \, °C$ ($104 \, °F$) at inland locations produced ozone concentrations greater than 290 ppb. This abnormally high photochemical activity enhanced the production of SOA. Atmospheric mixing was reduced by elevated temperatures aloft, trapping pollutants close to the earth's surface despite the hot ground-level temperatures. Measured 4 h average fine particle mass concentrations exceeded $86 \, \mu g \, m^{-3}$ (Fraser et al., 1996), with even greater concentrations predicted at sites that were not monitored. Air quality measurements used to support CMB calculations were made at Long Beach, central Los Angeles, Azusa, and Claremont. The location of these receptor sites is shown in Fig. 8. Long Beach is a coastal location on the leading (upwind) edge of the SoCAB. Central Los Angeles is highly impacted by fresh emissions from mobile sources traveling along the multiple freeways that converge on this location. Azusa and Claremont are progressively further inland locations that are influenced by the increased photochemical reaction of pollutants. All of the SoCAB receptor locations are highly urbanized, with intense emissions activity in and around the measurement sites.

The broad range of meteorological and emissions conditions experienced at locations in the two different air basins during the air quality episodes described above will provide an extensive test of the agreement between the UCD/CIT and CMB modeling approaches for fine particulate matter concentrations.

4. Comparison methods

A direct comparison of PM source apportionment estimates made by the CMB and UCD/CIT models is complicated because (1) previous CMB model studies have reported results for either particulate organic carbon or particulate total organic mass while the UCD/CIT model always uses total organic mass, (2) the averaging time used for CMB calculations may extend over the entire monitoring period for an air quality episode, while the UCD/CIT model requires at least one day of initialization time, and (3) the CMB model uses measurements at a single point while the UCD/CIT model averages concentrations within a grid cell with horizontal dimensions of 4–5 km. In the current study, source apportionment data was transformed to a common basis to facilitate the most direct comparison possible.

CMB model results for PM2.5 organic carbon concentrations in the SJV on 4–6 January 1996 were converted to total organic mass so that they can be compared to UCD/CIT source contribution predictions. The total organic mass concentration includes the mass of organic carbon plus the mass of other elements contained in organic molecules (oxygen, hydrogen, etc.). Conversion factors ranging between 1.4 and 2.1 have been used for this transformation in previous studies (Turpin and Lim, 2001). Higher conversion factors are generally used during periods of intense photochemical activity. Photochemical activity during the January episode considered in this study was very low; peak ozone concentrations were less than 50 ppb in the SJV on 4–6 January. For the ensuing analysis, all source contributions to organic carbon concentrations predicted by the CMB model were converted to total organic mass using a factor of 1.4. CMB results for the SoCAB on 8–9 September 1993 were expressed on a total organic mass basis, and so no additional conversion was needed.

The CMB source apportionment analysis for the SJV was based on samples collected over 72 h (4–6 January 1996) while the analysis for the SoCAB was based on samples collected over 48 h (8–9 September). The UCD/CIT grid model calculations were conducted for 72 h of model simulation for both episodes (SJV, 4–6 January; SoCAB, 7–9 September). Photochemical grid models typically require some initialization period during which radical species (not directly emitted or specified as a boundary condition) are produced by the chemical mechanism and model initial conditions are advected

out of the study region. Given the high emission rates and intense photochemical activity during the SoCAB episode, the grid model simulation was effectively initialized during the first simulated day (7 September) allowing for the direct comparison of the UCD/CIT and CMB model results over the 8–9 September time period without data conditioning. Pollutant emission rates and photochemical activity during the SJV episode were considerably less than those observed during the SoCAB study. The net effect of these two differences is that the UCD/CIT simulation of the SJV episode required more initialization time to ensure that source apportionment calculations were not dominated by initial conditions. Calculations show that UCD/CIT model was effectively initialized for the urban locations in the SJV after two simulated days (4–5 January) allowing for a comparison to CMB calculations on 6 January. PM10 concentrations at select SJV sampling sites varied by more than $100 \, \mu g \, m^{-3}$ over the period 4–6 January, resulting in a dataset that could not be considered statistically stationary with respect to time. Even though the magnitude of the PM concentrations varied significantly with time, UCD/CIT grid model results indicate that the percentage of the mass signal associated with each source-apportionment category was relatively time-invariant. Consistent with these observations, SJV CMB concentrations were scaled by the ratio of PM mass measured on 6 January to the mass measured over the 72 h sampling period to allow for direct comparison with the last 24 h of UCD/CIT grid model predictions. The ratio of 24-h average PM2.5 total mass concentrations to 72-h average PM2.5 total mass concentrations was measured to be 1.63, 1.17, and 1.27 at Fresno, Kern Wildlife Refuge, and Bakersfield, respectively.

CMB source-apportionment calculations are based on measurements made at a single point, whereas UCD/CIT model calculations represent a volume-average of the lowest grid cell coincident with the sampling site. For example, the SJV domain was discretized into 4 km square cells with the depth of the lowest layer set to 39 m resulting in a grid cell volume of approximately $\frac{2}{3}$ of a cubic kilometer. The ability of a single measurement to represent concentrations throughout such a large sample volume depends on the homogeneity of nearby meteorological and emissions fields as explained by Blanchard et al. (1999). Thus, receptor- and grid-based methods to calculate PM source-apportionment are expected to be consistent only to the extent at which nearby meteorological and emissions fields are homogeneous.

5. Results

Fig. 1 shows the 24 h average size distribution of airborne particulate matter predicted by the UCD/CIT airshed model at Fresno on 6 January 1996 (panel a) and at Azusa on 9 September 1993 (panel b). The Fresno and Azusa sites were chosen for the current example because CMB source apportionment calculations were carried out at these locations. The size distribution at each location shows primary contributions from the different externally mixed source classes that are resolved by the UCD/CIT air quality model. The amount of secondary organic material, sulfate, ammonium ion, and nitrate that accumulated on these primary particles is graphed separately. Secondary ammonium nitrate concentrations are predicted to be very significant at Fresno, with little or no contribution from SOA. In contrast, SOA concentrations at Azusa are much larger, with a smaller amount of particulate nitrate. These trends reflect the emissions and meteorological conditions in the SJV and the SoCAB during the air quality episodes under consideration (Held et al., 2004; Ying and Kleeman, submitted for publication). Previous studies have revealed the source-origin of this secondary material (Mysliwiec and Kleeman, 2002; Ying et al., submitted for publication); the current manuscript will focus on the source apportionment of primary particulate matter.

The airborne particle size distribution at both Fresno and Azusa appears bimodal, with the larger mode in the submicron range, and a smaller mode in the coarse particle range. The size distribution of particulate matter with aerodynamic diameter greater than 2.5 μm is dominated by paved road dust and crustal material other than paved road dust at both locations. Very little secondary particulate matter accumulates on these particles. The tail of this coarse particle size distribution extends into the accumulation mode, but does not dominate in this size range. At sizes smaller than 2.5 μm, contributions from combustions sources become significant. Wood smoke is predicted to account for the majority of the primary PM2.5 mass at Fresno, with smaller contributions from food cooking, diesel engines, and gasoline engines (non-catalyst). At Azusa, primary PM2.5 is more evenly distributed between diesel engines, gasoline engines (catalyst and non-catalyst), food cooking, and combustion of fuel with high sulfur content. Results of this type can be generated for each grid cell in the study domain at each hour of the UCD/CIT model simulation to support source apportionment calculations.

Table 1 shows predicted source contributions to PM2.5 concentrations at Fresno, Kern Wildlife Refuge, and Bakersfield on 6 January 1996 calculated using the UCD/CIT airshed model. The first column associated with each receptor location shows the predicted concentration of particulate matter mass associated with each source category including the amount of secondary particulate matter that has accumulated onto primary particle cores in the atmosphere. The second and third columns associated with each receptor location shows the primary particle mass and primary total organic
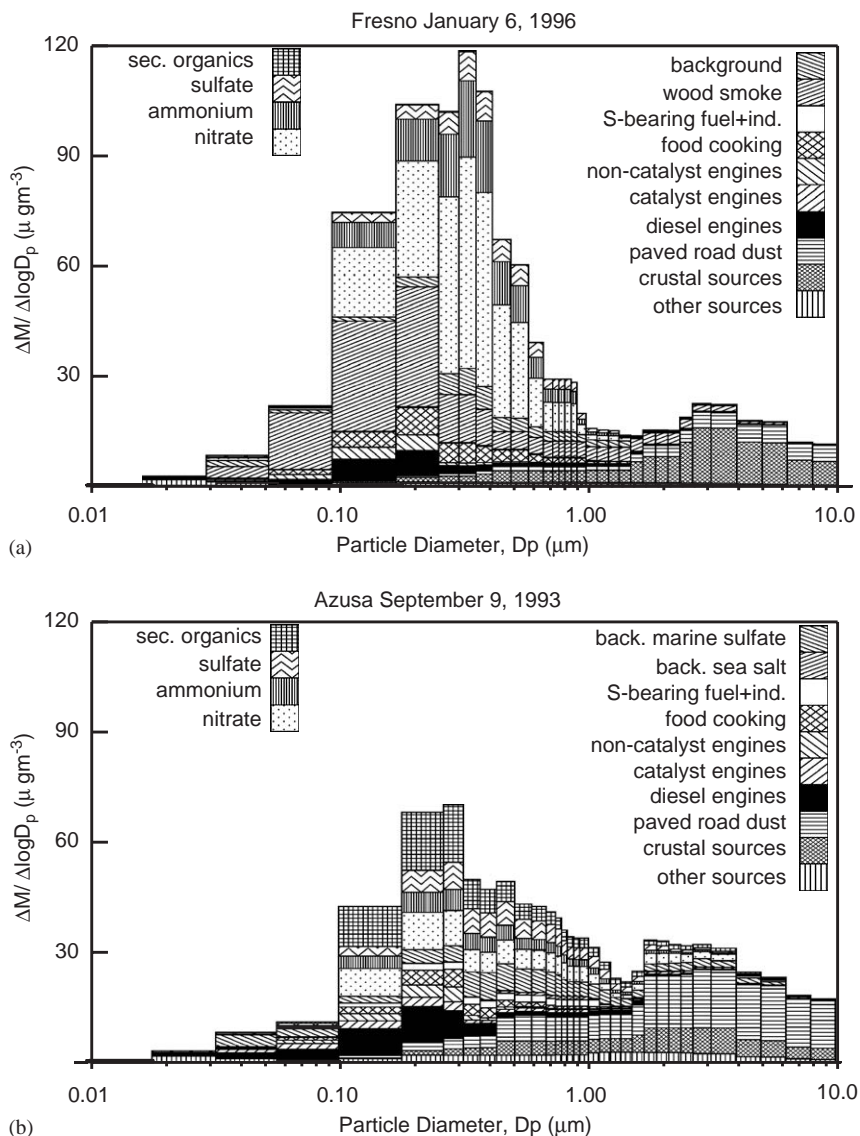
Fig. 1. Source contributions to the 24 h average size distribution of airborne particulate matter at Fresno (panel a) and Azusa (panel b) predicted by the UCD/CIT source-oriented air quality model.

mass concentrations associated with each source category. The fourth column associated with each receptor location shows the secondary organic aerosol that has accumulated onto primary particle cores released from each source category. The source origin of the secondary particulate matter was not identified in the current study. The results summarized in Table 1 show that wood smoke particles are predicted to account for $24 \,\mu g\,m^{-3}$ of primary particulate matter at Fresno. The majority of this primary wood smoke is organic material. Other predicted sources of primary PM2.5 at Fresno include food cooking ($6 \,\mu g\,m^{-3}$), crustal material

($4 \,\mu g\,m^{-3}$), diesel engine exhaust ($3 \,\mu g\,m^{-3}$), and gasoline engine exhaust (non-catalyst) ($2 \,\mu g\,m^{-3}$). Predicted source contributions to primary airborne PM2.5 concentrations at Bakersfield are similar to those at Fresno. Wood smoke dominates the primary PM2.5 concentration ($27 \,\mu g\,m^{-3}$) with smaller contributions from crustal material other than paved road dust ($7 \,\mu g\,m^{-3}$), diesel engines ($6 \,\mu g\,m^{-3}$), and gasoline engines ($3 \,\mu g\,m^{-3}$). Predicted concentrations at Kern Wildlife Refuge are much lower, reflecting the remote nature of this site. Notably absent at this location is a significant contribution from wood smoke. The only resolved primary

Table 1
PM2.5 source apportionment at three SJV locations averaged over 6 January 1996 using the UCD/CIT grid model

Source type	Fresno				Kern Wildlife Refuge				Bakersfield			
	Mass[a]	Prim.[b]	POA[c]	SOA[d]	Mass[a]	Prim.[b]	POA[c]	SOA[d]	Mass[a]	Prim.[b]	POA[c]	SOA[d]
Crustal material	3.98	3.83	0.25	0.00	2.20	2.03	0.12	0.00	7.06	6.84	0.53	0.00
Paved road dust	1.66	1.59	0.26	0.00	0.54	0.51	0.08	0.00	0.94	0.89	0.15	0.00
Diesel engines	3.62	3.31	0.53	0.00	0.85	0.71	0.09	0.00	6.73	6.27	0.91	0.00
Gasoline engines (non-catalyst)	2.39	2.12	1.83	0.00	0.27	0.18	0.15	0.00	3.42	2.99	2.58	0.00
Gasoline engines (catalyst)	0.34	0.30	0.19	0.00	0.04	0.03	0.02	0.00	0.46	0.41	0.26	0.00
Wood smoke	26.03	24.15	14.13	0.02	0.81	0.50	0.29	0.00	28.19	26.77	15.62	0.01
Meat cooking	6.82	6.43	4.61	0.00	0.10	0.05	0.04	0.00	2.25	2.14	1.58	0.00
High sulfur fuel combustion	0.42	0.14	0.03	0.00	0.21	0.08	0.02	0.00	0.19	0.10	0.02	0.00
Other	2.58	1.85	0.89	0.00	0.64	0.50	0.14	0.00	8.72	7.48	6.97	0.00
Background	41.56	4.33	2.99	0.12	44.92	7.22	5.29	0.39	54.08	4.94	3.14	0.37
Total	89.40	48.05	25.71	0.15	50.57	11.81	6.24	0.39	112.03	58.84	31.76	0.38

[a]Mass of primary particles and secondary material that has accumulated on those primary particles. Includes primary aerosol (Prim), secondary organic aerosol (SOA) and secondary inorganic aerosol (not shown).
[b]Primary mass due to direct emissions. Includes primary organic aerosol (POA).
[c]Primary organic aerosol.
[d]Secondary organic aerosol.

Table 2
PM2.5 source apportionment at four Los Angeles locations averaged over 8–9 September 1993 using the UCD/CIT grid model

Source type	Long Beach				Downtown LA			
	Mass[a]	Prim.[b]	POA[c]	SOA[d]	Mass[a]	Prim.[b]	POA[c]	SOA[d]
Crustal material	0.80	0.77	0.03	0.01	2.93	2.80	0.12	0.07
Paved road dust	5.00	4.57	0.75	0.15	7.51	6.90	1.14	0.30
Diesel engines	7.66	5.39	1.46	1.79	7.84	6.35	2.19	0.74
Gasoline engines (non-catalyst)	1.96	1.35	1.16	0.28	2.32	1.58	1.36	0.45
Gasoline engines (catalyst)	1.72	1.32	0.83	0.15	2.48	1.89	1.20	0.30
Meat cooking	1.21	0.82	0.60	0.14	4.63	3.48	2.57	0.65
High sulfur fuel	6.88	2.90	0.36	0.20	5.58	2.88	0.64	0.40
Other	6.34	5.43	3.79	0.11	4.37	3.88	1.53	0.16
Background sea salt	1.72	0.58	0.00	0.00	1.65	0.48	0.00	0.00
Background marine sulfate	15.53	5.73	0.58	0.44	15.64	6.85	0.93	0.91
Total	48.81	28.86	9.56	3.28	54.94	37.10	11.67	3.98
	Azusa				Claremont			
Crustal material	3.53	3.28	0.14	0.15	4.45	3.88	0.17	0.32
Paved road dust	7.52	6.56	1.08	0.59	10.87	8.90	1.47	1.22
Diesel engines	7.35	5.05	1.70	1.33	11.99	6.66	2.18	2.76
Gasoline engines (non-catalyst)	3.10	1.63	1.41	0.99	5.99	2.48	2.14	2.22
Gasoline engines (catalyst)	3.05	1.96	1.24	0.68	5.69	3.04	1.92	1.55
Meat cooking	4.03	2.37	1.75	0.99	6.27	2.88	2.12	2.06
High sulfur fuel	3.40	1.55	0.33	0.50	4.69	1.79	0.39	0.84
Other	3.26	2.63	0.94	0.32	5.13	3.65	1.16	0.75
Background sea salt	1.51	0.40	0.00	0.00	1.37	0.33	0.00	0.01
Background marine sulfate	17.23	7.49	1.06	1.67	18.89	7.37	1.28	2.77
Total	53.98	32.92	9.64	7.22	75.34	40.98	12.83	14.51

[a]Mass of primary particles and secondary material that has accumulated on those primary particles. Includes primary aerosol (Prim), secondary organic aerosol (SOA) and secondary inorganic aerosol (not shown).
[b]Primary mass due to direct emissions. Includes primary organic aerosol (POA).
[c]Primary organic aerosol.
[d]Secondary organic aerosol.

source contribution greater than $1 \mu g\, m^{-3}$ at Kern Wildlife Refuse is crustal sources other than paved road dust $(2 \mu g\, m^{-3})$ that is associated with windblown agricultural dust.

Contributions from background particles to PM2.5 mass shown in Table 1 are defined to originate from outside the model domain or before the start of the model simulation. The size of the model domain and/or the length of the model simulation could be increased to resolve these source contributions if they were significant. At Fresno and Bakersfield, background particles account for less than 10% of the total primary particle mass, and so they do not introduce significant uncertainty into source apportionment calculations. At Kern Wildlife Refuge background particles account for over half of the predicted primary particle mass, and so the source apportionment of primary particulate matter has high uncertainty. The concentration of primary particulate matter at this location is minor, however, and so the extra effort needed to resolve these source contributions is not worthwhile.

Table 2 shows predicted source contributions to PM2.5 concentrations at Long Beach, central Los Angeles, Azusa, and Claremont averaged over 8–9 September 1993 with a format analogous to Table 1. The dominant sources of primary PM2.5 mass at all locations are paved road dust $(5–9 \mu g\, m^{-3})$, diesel engines $(5–7 \mu g\, m^{-3})$, and gasoline engines (catalyst and non-catalyst) $(3–6 \mu g\, m^{-3})$ with smaller contributions from the combustion of fuel with high sulfur content $(1–3 \mu g\, m^{-3})$.

The results summarized in Tables 1 and 2 show that predicted primary PM2.5 concentrations in the urban areas of the SJV (Fresno and Bakersfield) are larger than primary PM2.5 concentrations at inland locations in the SoCAB (central LA, Azusa, and Claremont) by a factor of 1.17–1.79. The additional wood smoke predicted to be in the atmosphere in the SJV during the winter episode accounts for the majority of the additional mass.

Figs. 2 and 3 compare source contributions predicted by the UCD/CIT air quality model (Held et al., 2004) and the CMB statistical approach using organic tracers
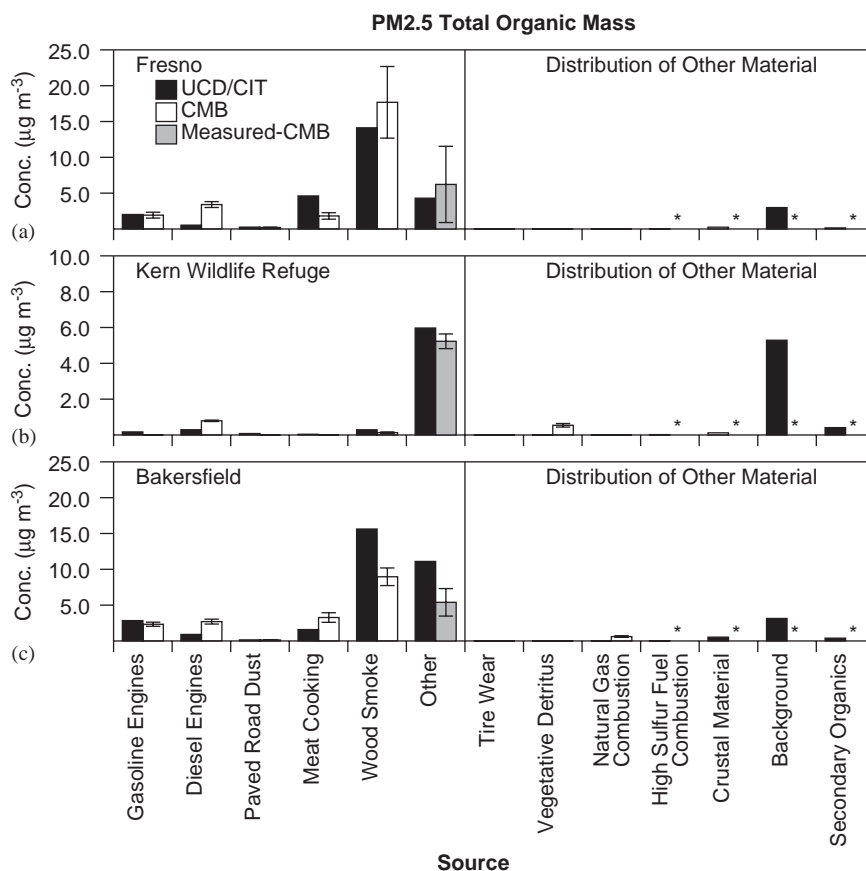

Fig. 2. Predicted source contributions to 24 h average PM2.5 total organic mass at Fresno (panel a), Kern Wildlife Refuge (panel b) and Bakersfield (panel c) on 6 January 1996. Predicted source contributions to secondary species are not shown. CMB model results are estimated based on the variation of 24 h average PM2.5 mass concentrations on 4–6 January 1996. Sources marked with a * were not resolved by the CMB model.
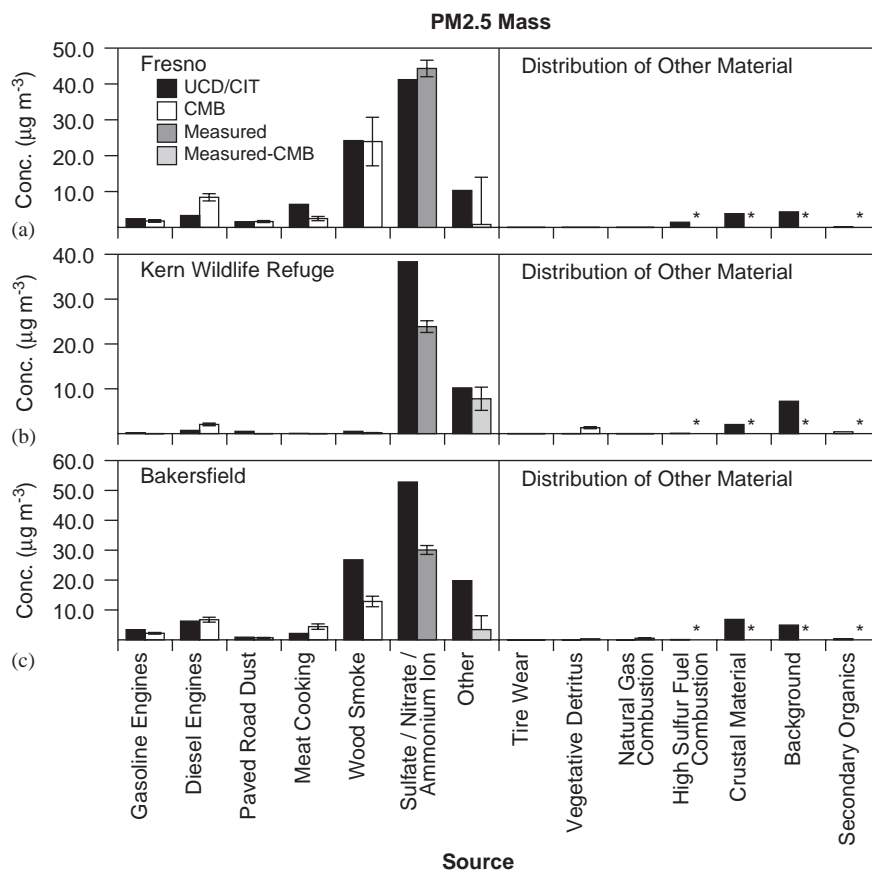
PM2.5 Mass

Fig. 3. Predicted source contributions to 24 h average PM2.5 mass at Fresno (panel a), Kern Wildlife Refuge (panel b) and Bakersfield (panel c) on 6 January 1996. Predicted source contributions to secondary species are not shown. CMB model results are estimated based on the variation of 24 h average PM2.5 mass concentrations on 4–6 January 1996. Sources marked with a * were not resolved by the CMB model.

(Schauer and Cass, 2000) at different locations in the SJV on 6 January 1996. CMB source contributions for 4–6 January 1996 were scaled by the ratio of PM2.5 mass measured on 6 January to PM2.5 mass measured on 4–6 January as discussed in the previous section. Major sources that are common to both the UCD/CIT and CMB approaches are grouped on the left side of each figure, while minor sources are grouped on the right. Both the UCD/CIT air quality model and the CMB approach calculate that wood smoke is the largest source of primary PM2.5 at urban locations (Fresno and Bakersfield) in the SJV during the winter air quality episode studied here. The models also show reasonable agreement for calculated primary contributions from gasoline engines, diesel engines, paved road dust, and meat cooking at these urban sites. At the rural Kern Wildlife Station, both the UCD/CIT and CMB models calculate that primary PM2.5 concentrations are very low. Fig. 3 shows that the amount of sulfate, nitrate, and

ammonium ion predicted by the UCD/CIT air quality model is in good agreement with measurements at all three locations during this episode. The PM2.5 material other than gasoline engines, diesel engines, paved road dust, meat cooking, and wood smoke in the UCD/CIT air quality model is plotted in the "other" category in Figs. 2 and 3. SOA is also included in the UCD/CIT "other" category. The difference between measured PM2.5 concentrations and the source contributions resolved by the CMB model are plotted alongside this "other" material. Agreement between predicted and observed concentrations of "other" material is reasonable given the assumptions that were necessary to directly compare the models. The UCD/CIT calculation predicts that the majority of the "other" PM2.5 material in the SJV is actually background particles that either originated outside the study domain or before the start of the 3-day model episode. This result suggests that upwind sources with unknown composition may
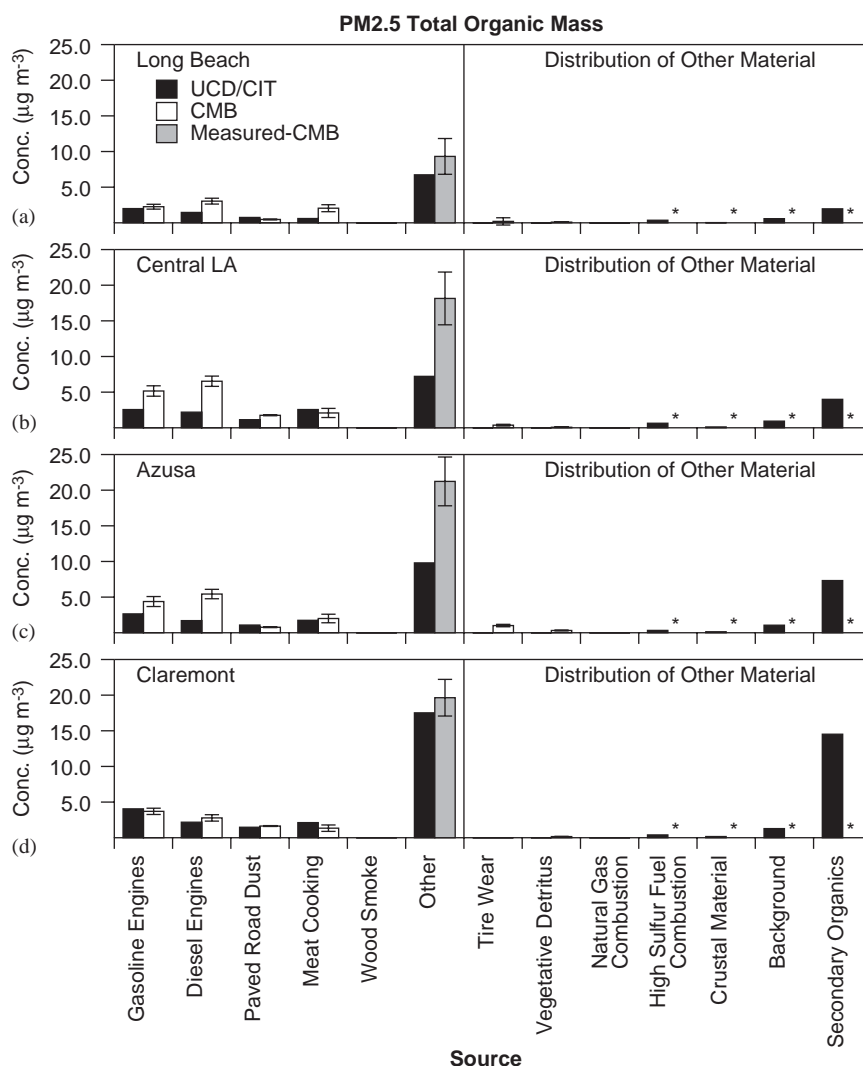
PM2.5 Total Organic Mass

Fig. 4. Predicted source contributions to 24 h average PM2.5 total organic mass at Long Beach (panel a), central Los Angeles (panel b), Azusa (panel c), and Claremont (panel d) on 8–9 September 1993. Predicted source contributions to secondary species are not shown. Sources marked with a * were not resolved by the CMB model.

account for several $\mu g\,m^{-3}$ of PM2.5 in the SJV during the winter months, or that some of the organic tracers used by the CMB model may not be stable over periods longer than 3 days. SOA production in the UCD/CIT model is estimated to be very low during the winter episode (see Table 1) because photochemical activity is close to an annual minimum.

Figs. 4 and 5 compare source contributions to the PM2.5 total organic mass concentrations and PM2.5 mass concentrations calculated by the UCD/CIT air quality model (Ying and Kleeman, submitted for publication) and the CMB statistical approach using organic tracers (Schauer et al., 2002a, b, c) at different locations in the SoCAB on 8–9 September 1993. The format used for these figures is analogous to Figs. 2 and 3 described above. Both the UCD/CIT and the CMB models calculate that the dominant sources of primary PM2.5 are gasoline engines, diesel engines, paved road dust, and meat cooking. The agreement between primary source contribution estimates made by the UCD/CIT and CMB models at Claremont is excellent. Calculated CMB source contributions to PM2.5 mass from diesel engines are higher than UCD/CIT predictions at Long Beach, central Los Angeles, and Azusa. Previous studies have observed that the UCD/CIT model under-predicts concentrations of elemental carbon, total organic mass, and NO_x by a factor of approximately 2 at these locations during the morning
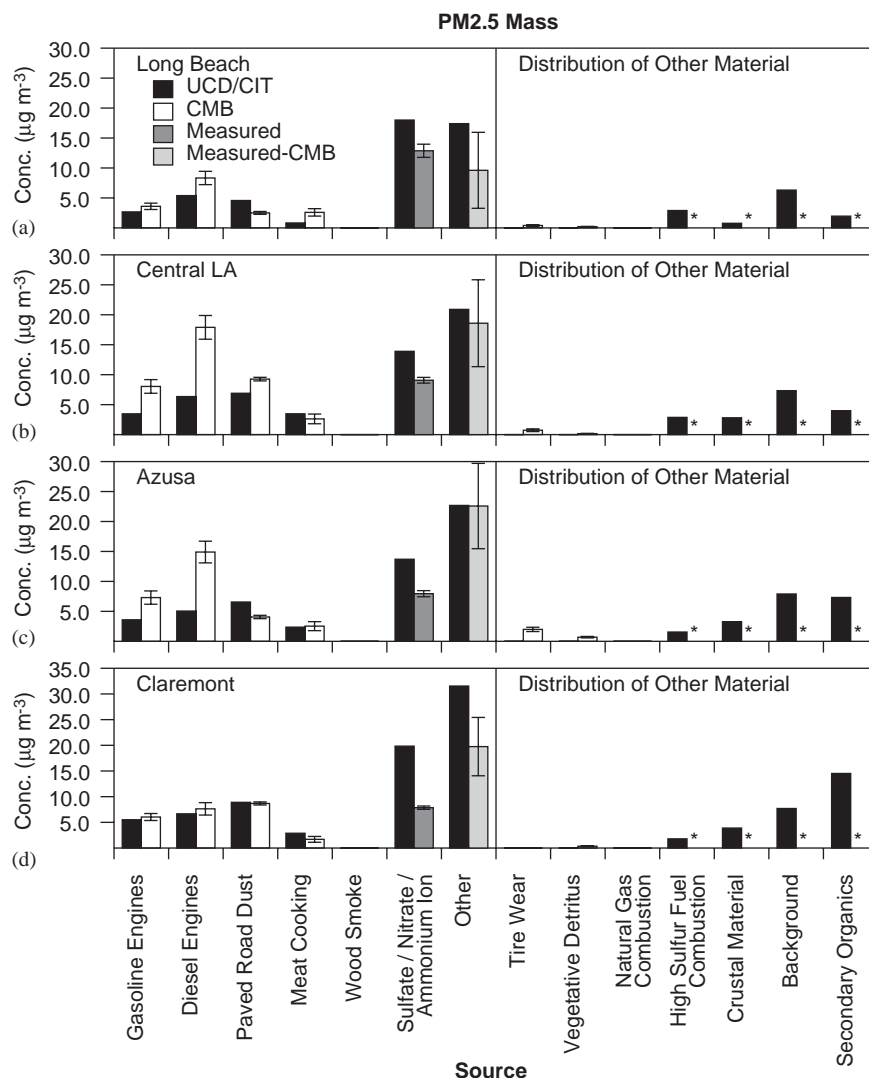
Fig. 5. Predicted source contributions to 24 h average PM2.5 mass at Long Beach (panel a), central Los Angeles (panel b), Azusa (panel c), and Claremont (panel d) on 8–9 September 1993. Predicted source contributions to secondary species are not shown. Sources marked with a * were not resolved by the CMB model.

rush hour period (concentrations at other times of the day are correct) (Ying and Kleeman, submitted for publication). The simultaneous under-prediction of elemental carbon, total organic mass, and NO_x suggests that the activity level of primary emissions from diesel-powered vehicles in the emissions inventory is biased low during the morning rush hour time period. The mobile source inventory that was available for the current study did not separately predict the spatial and temporal distribution of diesel-powered vehicles. Instead, a constant fraction of the total vehicle miles traveled in the SoCAB was apportioned to diesel-powered vehicles with the same spatial and temporal distribution as

emissions from gasoline-powered vehicles. It is expected that future emissions inventories produced for the SoCAB will use more realistic models of heavy-duty diesel-powered vehicle emissions.

Fig. 5 shows that the amount of sulfate, nitrate, and ammonium ion predicted by the UCD/CIT air quality model is slightly greater than the measured values at all receptor locations. The amount of "other" PM2.5 total organic mass is under-predicted by the UCD/CIT air quality model at all four receptor sites, while the amount of "other" PM2.5 mass is slightly over-predicted. The majority of the "other" organic material is SOA with predicted concentrations increasing at inland locations.

The predicted 48-h average SOA concentration at Claremont on 8–9 September 1993 was $14.5\,\mu g\,m^{-3}$. This large SOA concentration results from the high photochemical activity during the 7–9 September period. Background material originating from locations upwind of the model domain accounts for the majority of the "other" PM2.5 mass signal at Long Beach, central Los Angeles, and Azusa. Smaller contributions are also predicted for crustal material and for sources that burn fuel with high sulfur content. Organic tracer source profiles have not been measured for these sources and so they cannot be resolved by CMB calculations.

Fig. 6 illustrates a scatter plot of source contributions to PM2.5 primary total organic mass concentrations (panel a) and PM2.5 primary mass concentrations (panel b) for Fresno, Kern Wildlife Refuge, and Bakersfield on 6 January 1996, and Long Beach, central Los Angeles, Azusa, and Claremont on 8–9 September 1993. The vertical axis of each plot shows the source contribution predicted by the UCD/CIT air quality model, while the lower axis of each plot shows the source contribution calculated by the CMB calculation. The slope of the correlation line fitted through the data is 0.84 for total organic mass and 0.83 for all mass, with a correlation coefficient (R^2) of 0.7 for total organic mass and 0.55 for all mass. The regression statistics

Fig. 6. Correlation between CMB and UCD/CIT estimates for (a) PM2.5 total organic mass and (b) PM2.5 total mass. Closed symbols correspond to the SoCAB while open symbols correspond to the SJV. Wood smoke was only found in the SJV.

shown in Fig. 6 are influenced most heavily by dominant sources. To consider all sources equally, the ratios of all the UCD/CIT to CMB source contributions shown in Fig. 6 were averaged without weighting by CMB mass. The average ratio of UCD/CIT to CMB source contributions was 0.93 for PM2.5 total organic mass and 1.06 for PM2.5 total mass. This metric illustrates the level of agreement between the two source apportionment techniques independent of the source strength. Overall, this analysis shows very good agreement between UCD/CIT model predictions in a grid cell with dimensions of 4–5 km vs. CMB model calculations based on point measurements of airborne particle composition.

As discussed previously, the CIT/UCD air quality model predicts source contributions to primary and secondary particulate matter at all locations in the study domain. This feature is useful for exposure studies that seek to quantify the environmental impact of airborne particulate matter. Figs. 7 and 8 show the predicted regional source contributions to primary PM2.5 concentrations in the SJV on 6 January 1996, and in the SoCAB on 9 September 1993. Fig. 7a shows that 24 h average primary PM2.5 concentrations in the SJV are predicted to peak at approximately $48\,\mu g\,m^{-3}$ in the region surrounding Fresno and $62\,\mu g\,m^{-3}$ in the region surrounding Bakersfield. The majority of this material is wood smoke (Fig. 7b), with peak concentrations from this source exceeding $30\,\mu g\,m^{-3}$. Particulate matter released from food cooking (Fig. 7e) is also concentrated around the urban centers, with peak concentrations reaching $6\,\mu g\,m^{-3}$. Particles originally released from gasoline engines (catalyst—Fig. 7i and non-catalyst equipped—Fig. 7g) are concentrated along transportation corridors (Interstate 5 and California State Highway 99) that connect the major urban centers. Particles originally released from diesel engines (Fig. 7d) have a more uniform concentration of approximately $2\,\mu g\,m^{-3}$ across a significant portion of the SJV with peak concentrations exceeding $8\,\mu g\,m^{-3}$ in Bakersfield. The distribution of paved road dust (Fig. 7h) and crustal material other than paved road dust (Fig. 7c) is broader, with significant concentrations in rural areas. Finally, the primary particulate matter associated with the combustion of fuel with high sulfur content (Fig. 7f) is isolated to a single location, with a peak concentration of approximately $10\,\mu g\,m^{-3}$. This results from a large point source in this region, and suggests that monitoring should be established to measure the impact of this point source.

Fig. 8a shows that 24 h average primary PM2.5 concentrations in the SoCAB are predicted to peak at approximately $45\,\mu g\,m^{-3}$ in the eastern portion of the air basin. Transportation sources (paved road dust—Fig. 8a, diesel engines—Fig. 8d, catalyst-equipped gasoline engines—Fig. 8f, and non-catalyst-equipped
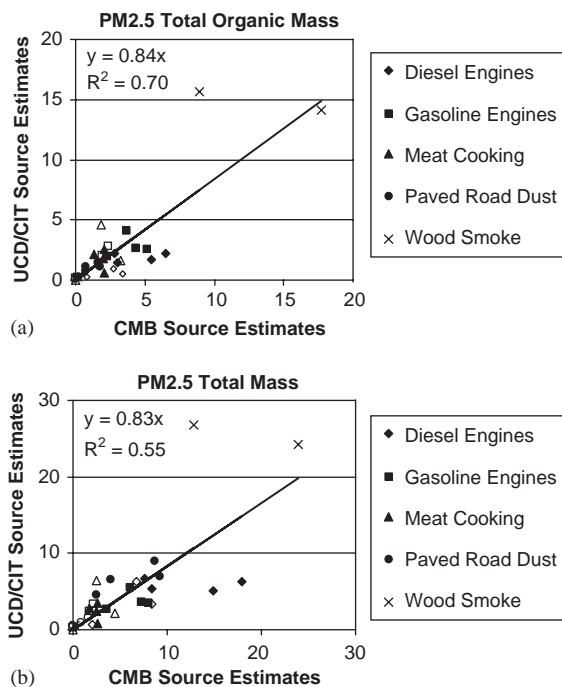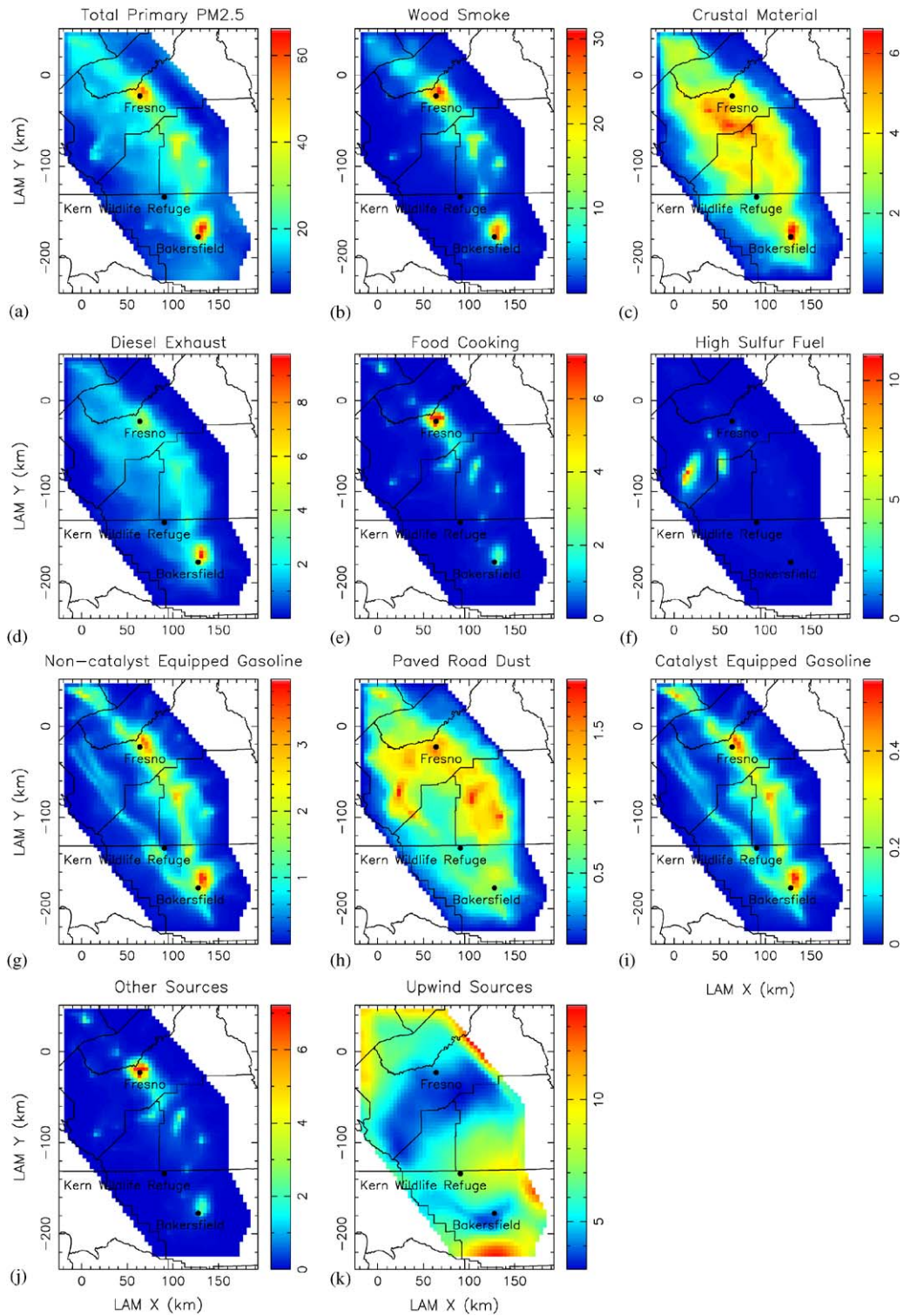
Fig. 7. Regional distribution of primary PM2.5 mass predicted by the UCD/CIT air quality model in the San Joaquin Valley on 6 January 1996. Units are $\mu g\,m^{-3}$.
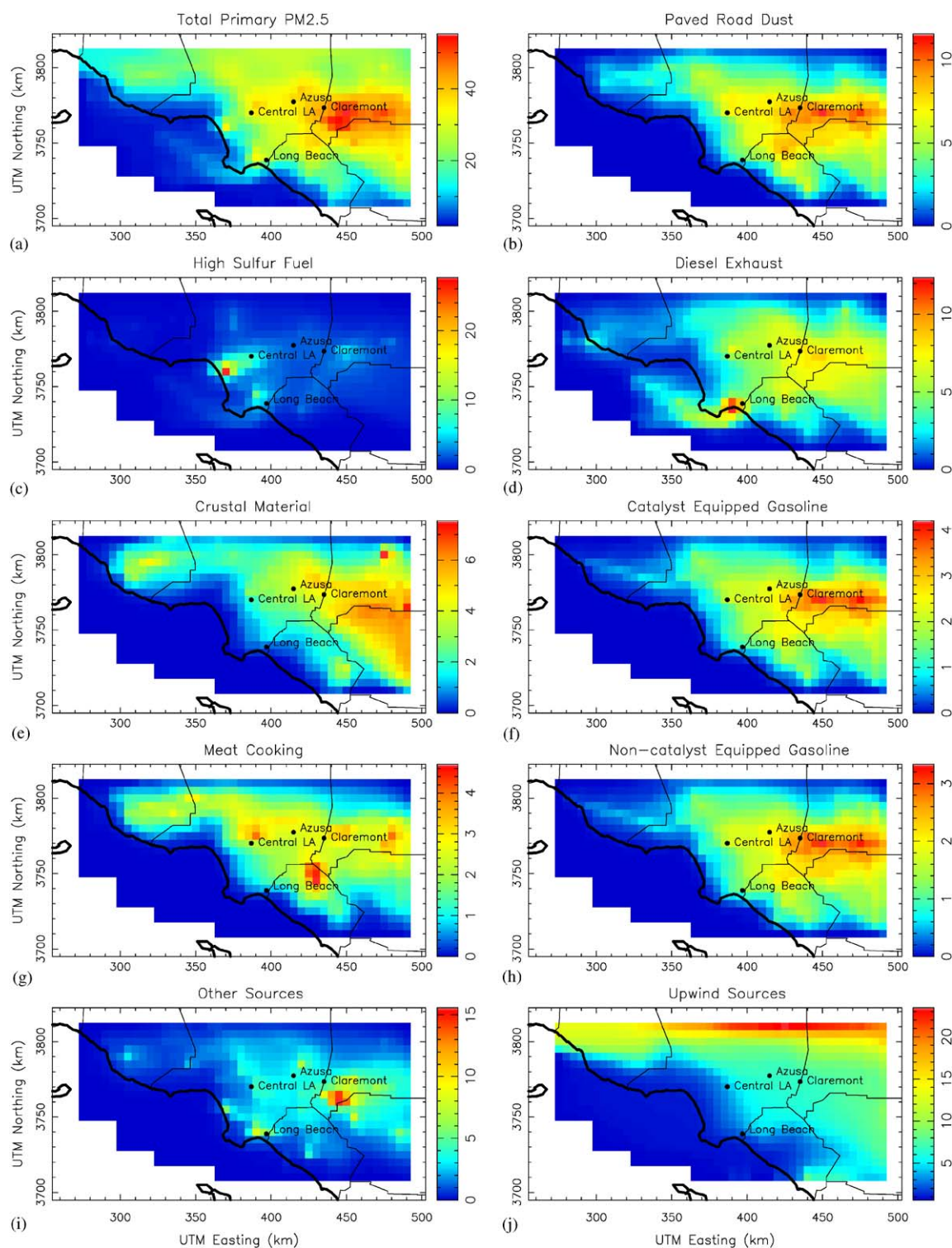
Fig. 8. Regional distribution of primary PM2.5 mass predicted by the UCD/CIT air quality model in the South Coast Air Basin on 9 September 1993. Units are $\mu g\,m^{-3}$.

gasoline engines—Fig. 8h) account for the majority of the primary PM2.5 mass, with broad geographical distribution. The combustion of fuel with high sulfur content (Fig. 8c) at the Los Angeles International Airport and the port of Los Angeles contributes primary PM2.5 concentrations reaching $25 \, \mu g \, m^{-3}$ in the vicinity around these locations. As discussed previously, this material accounts for a significant fraction of the primary PM2.5 mass that cannot be resolved by CMB source apportionment calculations during the 7–9 September 1993 episode. The distribution of primary crustal PM2.5 mass (Fig. 8e) is highest in the eastern portion of the SoCAB, while the primary food cooking particles are concentrated further east.

Overall, the regional distribution of primary PM2.5 illustrated by Figs. 7 and 8 is useful for the identification localized "hotspots" of particulate air pollution that may not currently have monitoring sites associated with them. The regional distribution predictions are also useful for source exposure calculations.

6. Conclusions

A direct comparison was made between predictions for source contributions to airborne particulate matter made by the UCD/CIT source-oriented externally mixed airshed model and the CMB model for two air quality episodes: the San Joaquin Valley (4–6 January 1996) and the South Coast Air Basin (7–9 September 1993). The results from the two independent source apportionment calculations show strong agreement for primary PM2.5 organics, with a correlation slope of 0.84 and a correlation coefficient (R^2) of 0.70. Agreement for primary PM2.5 mass was similarly good, with a correlation slope of 0.83 and a correlation coefficient (R^2) of 0.55. The agreement between the two models during air quality episodes with greatly different characteristics suggests that the formulation of the UCD/CIT air quality model is robust and that this model can yield accurate source apportionment results when supplied with proper input data.

The UCD/CIT air quality model identified several sources of primary PM2.5 mass that may explain residual material in the CMB calculation including combustion sources that burn fuel with high sulfur content (such as the Los Angeles International Airport and the port of Los Angeles), crustal material other than paved road dust, background particles released from unknown sources upwind of the air-basins, and particles that have aged in the atmosphere for more than 3 days. Source profiles should be developed for high-sulfur fuel combustion activities and monitors should be placed around these sources to verify the contributions that these sources make to PM2.5 concentrations. The regional distribution of primary PM2.5 material

predicted by the UCD/CIT air quality model can be used to support future exposure analysis studies that seek to quantify the environmental impact of airborne particulate matter released from different sources.

References

Abu-Allaban, M., Gertler, A., Lowenthal, D., 2002. A preliminary apportionment of the sources of ambient PM10, PM2.5, and VOCs in Cairo. Atmospheric Environment Part a—General Topics 36 (35), 5549–5557.

Aw, J., Kleeman, M.J., 2003. Evaluating the first-order effect of intraannual temperature variability on urban air pollution. Journal of Geophysical Research—Atmospheres 108(D12) Art. No. 4365.

Bae, M.S., Schauer, J.J., DeMinter, J.T., Turner, J.R., 2004. Hourly and daily patterns of particle-phase organic and elemental carbon concentrations in the urban atmosphere. Journal of the Air and Waste Management Association 54 (7), 823–833.

Blanchard, C.L., et al., 1999. Spatial representativeness and scales of transport during the 1995 Integrated Monitoring Study in California's San Joaquin Valley. Atmospheric Environment 33 (29), 4775–4786.

Butler, A.J., Andrew, M.S. and Russell, A.G., 2003. Daily sampling of PM2.5 in Atlanta: results of the first year of the assessment of spatial aerosol composition in Atlanta study. Journal of Geophysical Research—Atmospheres 108(D1) Art. No. 8415.

Carter, W.P.L., 1990. A detailed mechanism for the gas-phase atmospheric reactions of organic-compounds. Atmospheric Environment Part a—General Topics 24 (3), 481–518.

Chen, K.S., Lin, C.F., Chou, Y.M., 2001. Determination of source contributions to ambient PM2.5 in Kaohsiung, Taiwan, using a receptor model. Journal of the Air and Waste Management Association 51 (4), 489–498.

Chow, J.C., et al., 1992. Pm10 source apportionment in California San-Joaquin Valley. Atmospheric Environment Part a—General Topics 26 (18), 3335–3354.

Cooper, J.A., et al., 1989. Final appendix V-G, PM10 source composition library for the South Coast Air Basin. Technical Report, South Coast Air Quality Management District, Diamond Bar, California.

Fraser, M.P., Grosjean, D., Grosjean, E., Rasmussen, R.A., Cass, G.R., 1996. Air quality model evaluation data for organics. 1. Bulk chemical composition and gas/particle

distribution factors. Environmental Science and Technology 30 (5), 1731–1743.

Griffin, R.J., Dabdub, D., Seinfeld, J.H., 2002. Secondary organic aerosol—1. Atmospheric chemical mechanism for production of molecular constituents. Journal of Geophysical Research—Atmospheres 107(D17) Art. No. 4332.

Harley, R.A., Hannigan, M.P., Cass, G.R., 1992. Respeciation of organic gas emissions and the detection of excess unburned gasoline in the atmosphere. Environmental Science and Technology 26 (12), 2395–2408.

Harley, R.A., Russell, A.G., Cass, G.R., 1993. Mathematical-modeling of the concentrations of volatile organic-compounds—model performance using a lumped chemical mechanism. Environmental Science and Technology 27 (8), 1638–1649.

Held, T., Ying, Q., Kaduwela, A., Kleeman, M., 2004. Modeling particulate matter in the San Joaquin Valley with a source-oriented externally mixed three-dimensional photochemical grid model. Atmospheric Environment Part a—General Topics 38 (22), 3689–3711.

Hildemann, L.M., Markowski, G.R., Cass, G.R., 1991a. Chemical-composition of emissions from urban sources of fine organic aerosol. Environmental Science and Technology 25 (4), 744–759.

Hildemann, L.M., Markowski, G.R., Jones, M.C., Cass, G.R., 1991b. Submicrometer aerosol mass distributions of emissions from boilers, fireplaces, automobiles, diesel trucks, and meat-cooking operations. Aerosol Science and Technology 14 (1), 138–152.

Houck, J.E., et al., 1989. Determination of particle size distribution and chemical composition of particulate matter from selected sources in California. Technical Report, Contract A6-175-32, California Air Resources Board, OMNI Environment Service Incorporate, Desert Research Institute, Beaverton, Oregon.

Kim, B.M., Teffera, S., Zeldin, M.D., 2000a. Characterization of PM2.5 and PM10 in the South Coast Air Basin of southern California: Part 1—spatial variations. Journal of the Air and Waste Management Association 50 (12), 2034–2044.

Kim, B.M., Teffera, S., Zeldin, M.D., 2000b. Characterization of PM2.5 and PM10 in the South Coast Air Basin of southern California: Part 2—temporal variations. Journal of the Air and Waste Management Association 50 (12), 2045–2059.

Kleeman, M.J., Cass, G.R., 1998. Source contributions to the size and composition distribution of urban particulate air pollution. Atmospheric Environment 32 (16), 2803–2816.

Kleeman, M.J., Cass, G.R., 2001. A 3D Eulerian source-oriented model for an externally mixed aerosol. Environmental Science and Technology 35 (24), 4834–4848.

Kleeman, M.J., Schauer, J.J., Cass, G.R., 1999. Size and composition distribution of fine particulate matter emitted from wood burning, meat charbroiling, and cigarettes. Environmental Science and Technology 33 (20), 3516–3523.

Kleeman, M.J., Schauer, J.J., Cass, G.R., 2000. Size and composition distribution of fine particulate matter emitted from motor vehicles. Environmental Science and Technology 34 (7), 1132–1142.

Magliano, K.L., et al., 1999. Spatial and temporal variations in PM10 and PM2.5 source contributions and comparison to emissions during the 1995 integrated monitoring study. Atmospheric Environment 33, 4757–4773.

Modey, W.K., Eatough, D.J., 2004. Twenty four-hour PC-BOSS air-monitoring results from the NETL fine-particulate sampling site in Pittsburgh, Pennsylvania: an annual perspective. Aerosol Science and Technology 38 (3), 194–204.

Mysliwiec, M.J., Kleeman, M.J., 2002. Source apportionment of secondary airborne particulate matter in a polluted atmosphere. Environmental Science and Technology 36 (24), 5376–5384.

Odum, J.R., et al., 1996. Gas/particle partitioning and secondary organic aerosol yields. Environmental Science and Technology 30 (8), 2580–2585.

Pandis, S.N., Harley, R.A., Cass, G.R., Seinfeld, J.H., 1992. Secondary organic aerosol formation and transport. Atmospheric Environment Part a—General Topics 26 (13), 2269–2282.

Park, S.S., Bae, M.S., Kim, Y.J., 2001. Chemical composition and source apportionment of PM2.5 particles in the Sihwa area, Korea. Journal of the Air and Waste Management Association 51 (3), 393–405.

Pun, B.K., Griffin, R.J., Seigneur, C., Seinfeld, J.H., 2002. Secondary organic aerosol—2. Thermodynamic model for gas/particle partitioning of molecular constituents. Journal of Geophysical Research—Atmospheres 107(D17) Art. No. 4333.

Russell, M., Allen, D.T., Collins, D.R., Fraser, M.P., 2004. Daily, seasonal, and spatial trends in PM2.5 mass and composition in Southeast Texas. Aerosol Science and Technology 38, 14–26.

Schauer, J.J., Cass, G.R., 2000. Source apportionment of wintertime gas-phase and particle-phase air pollutants using organic compounds as tracers. Environmental Science and Technology 34 (9), 1821–1832.

Schauer, J.J., Kleeman, M.J., Cass, G.R., Simoneit, B.R.T., 1999a. Measurement of emissions from air pollution sources. 1. C-1 through C-29 organic compounds from meat charbroiling. Environmental Science and Technology 33 (15 May), 1566–1577.

Schauer, J.J., Kleeman, M.J., Cass, G.R., Simoneit, B.R.T., 1999b. Measurement of emissions from air pollution sources. 2. C-1 through C-30 organic compounds from medium duty diesel trucks. Environmental Science and Technology 33 (15 May), 1578–1587.

Schauer, J.J., Kleeman, M.J., Cass, G.R., Simoneit, B.R.T., 2001. Measurement of emissions from air pollution sources. 3. C-1–C-29 organic compounds from fireplace combustion of wood. Environmental Science and Technology 35 (1 May), 1716–1728.

Schauer, J.J., Fraser, M.P., Cass, G.R., Simoneit, B.R.T., 2002a. Source reconciliation of atmospheric gas-phase and particle-phase pollutants during a severe photochemical smog episode. Environmental Science and Technology 36 (17), 3806–3814.

Schauer, J.J., Kleeman, M.J., Cass, G.R., Simoneit, B.R.T., 2002b. Measurement of emissions from air pollution sources. 4. C-1–C-27 organic compounds from cooking

with seed oils. Environmental Science and Technology 36 (15 Feb), 567–575.

Schauer, J.J., Kleeman, M.J., Cass, G.R., Simoneit, B.R.T., 2002c. Measurement of emissions from air pollution sources. 5. C-1–C-32 organic compounds from gasoline-powered motor vehicles. Environmental Science and Technology 36 (15 Mar), 1169–1180.

Taback, H.J., Brienza, A.R., Macko, J. and Brunetz, N., 1979. Fine particle emissions from stationary and miscellaneous sources in the South Coast Air Basin. Technical Report, Contract A6-191-30, California Air Resources Board, KVB Incorporated, Research-Cottrell, Tustin, California.

Turpin, B.J., Lim, H.J., 2001. Species contributions to PM2.5 mass concentrations: revisiting common assumptions for estimating organic mass. Aerosol Science and Technology 35 (1), 602–610.

Vukovich, F.M., Sherwell, J., 2002. Comparison of fine particles and the relationship between particle variation and meteorology at an urban site and a remote site in the eastern United States. Journal of the Air and Waste Management Association 52 (5), 573–584.

Watson, J.G., Chow, J.C., 2002. A wintertime PM2.5 episode at the Fresno, CA. Supersite 36 (3), 465–475.

Watson, J.G., Chow, J.C., Fujita, E.M., 2001. Review of volatile organic compound source apportionment by chemical mass balance. Atmospheric Environment 35 (9), 1567–1584.

Watson, J.G., et al., 2002. Simulating changes in source profiles from coal-fired power stations: use in chemical mass balance of PM2.5 in the Mount Zirkel Wilderness. Energy and Fuels 16 (2), 311–324.

Wittig, A.E., et al., 2004. Pittsburgh air quality study overview. Atmospheric Environment Part a—General Topics 38 (20), 3107–3125.

Ying, Q., Kleeman, M. Verification of a source-oriented external mixture air quality model during a severe photochemical smog event. Atmospheric Environment Part a—General Topics, submitted for publication.

Ying, Q., Held, A.E., Kleeman, M.J. Source contributions to the regional distribution of secondary particulate matter in California. Environmental Science and Technology, submitted for publication.

Zheng, M., Cass, G.R., Schauer, J.J., Edgerton, E.S., 2002. Source apportionment of PM2.5 in the southeastern United States using solvent-extractable organic compounds as tracers. Environmental Science and Technology 36 (11), 2361–2371.